ORGANIC CHEMISTRY FRONTIERS

RESEARCH ARTICLE

View Article Online
View Journal | View Issue

Cite this: *Org. Chem. Front.*, 2025, **12**, 2266

A superior and accessible cavitand receptor for the binding of monoterpenes and sesquiterpenes in water†

Hugo Marchi Luciano,‡[a] Ricard López-Coll,‡[a] Rubén Álvarez-Yebra[a] and Agustí Lledó *[a,b]

Received 22nd January 2025,
Accepted 4th February 2025

DOI: 10.1039/d5qo00161g

rsc.li/frontiers-organic

A water-soluble receptor based on resorcin[4]arene featuring 8 solubilising carboxylate units (**BC4**) has been obtained in a straightforward manner without chromatographic purifications. **BC4** is soluble in water in a wide range of pH, and is able to accommodate guests of different sizes and shapes, including monoterpenes and sesquiterpenes, providing enhanced binding capabilities with respect to previously reported analogues. The molecular recognition events within **BC4** are sensitive to subtle changes in guest shape and size, as illustrated by disparate exchange kinetics observed among the guests tested.

Introduction

Water soluble synthetic receptors are the quintessential example of bioinspired hosts and have great potential in the development of bioinspired catalysis or sensing devices for analyte detection in biological media.[1,2] The binding of organic molecules in aqueous media benefits from the hydrophobic effect, resulting in better binding abilities for a given water soluble host in relation to lipophilic analogues operating in organic media, where competitive binding by solvent molecules is significant. Cavitand receptors based on resorcin[4]arenes and featuring benzimidazole panels were first introduced by Rebek and co-workers and constitute a particularly interesting subset of hosts for studies in aqueous media (Fig. 1).[3] The benzimidazole units are placed at the appropriate distance and orientation to establish hydrogen bonds with bridging water molecules, stabilizing the binding competent closed form of the cavitand (the so-called *vase* conformation) by means of an uninterrupted hydrogen bond network. In contrast, the *vase* form is typically disrupted by protic solvents in other cavitand scaffolds, making them less appealing for applications in water.[4] Benzimidazole-type cavitands (**BC**) are rendered water-soluble by addition of solubilizing groups at either the upper rim[5–8] or the feet of the resorcin[4]arene core.[9–11] Of the two approaches, the former is the most straightforward from a synthetic point of view, allowing the preparation of sizable amounts of cavitands without chromatographic purifications in five steps from resorcinol (Fig. 1a). This accessibility has popularized such receptors for a range of applications specially in sensing,[12–19] but also in catalysis[20] and *trans*-membrane transport.[21] The use of arrays of **BC** receptors as highly sensitive and selective sensory systems has proved particularly useful.[12–14,16–18] Despite this demonstrated utility, only a reduced set of water-soluble upper rim functionalized **BCs** has been developed (**BC1–3**, Fig. 1b), all suffering from a limited operative range of pH (either basic or acidic). With these limitations in mind and given our interest in developing containers for binding biologically relevant molecules,[22] we set out to develop an improved **BC** host with a deeper hydrophobic pocket and an enhanced solubility profile. We report here the synthesis of this new receptor **BC4** and its binding capabilities against a set of terpenes and alkaloids (Fig. 1c).

Results and discussion

While **BC**-type receptors can be easily synthesized from octanitro precursor **1** (Scheme 1), the diversification of the structure is not trivial given the impossibility to purify the (highly polar) reaction intermediates by chromatography, and the reduced number of functional imidate precursors available. As a result, only four different benzimidazole cavitands with functional groups suitable for further elaboration have been described.[5–8,23] We envisaged that imidate **3** would be accessi-

[a]*Institut de Química Computacional i Catàlisi (IQCC), Universitat de Girona, Maria Aurèlia Capmany 69, 17003 Girona, Spain. E-mail: agusti.lledo@udg.edu*
[b]*Institute of Chemical Research of Catalonia (ICIQ), The Barcelona Institute of Science and Technology, Av. Països Catalans 16, 43007 Tarragona, Spain*

†Electronic supplementary information (ESI) available: Synthesis and characterization data for **3**, **4**, **BC4**. Copies of NMR and HRMS spectra for all new compounds. Spectroscopic and computational data supporting this work are available from the CORA RDR repository. See DOI: **https://doi.org/10.1039/d5qo00161g**

‡These authors contributed equally.

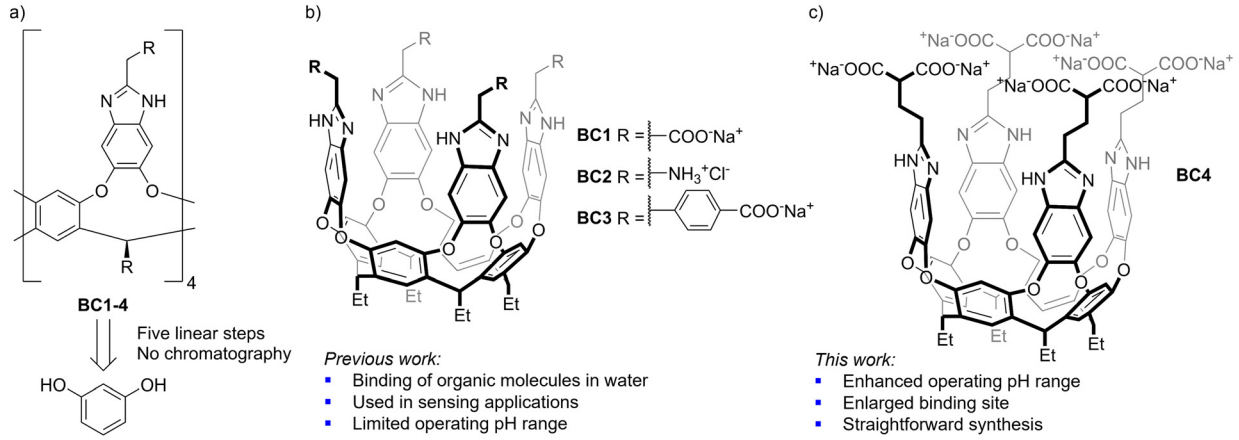

Fig. 1 (a) Schematic structure and retrosynthesis of water soluble benzimidazole cavitands (**BC**). (b) Previously reported **BC** receptors. (c) Newly developed octacarboxylate **BC** receptor **BC4**.

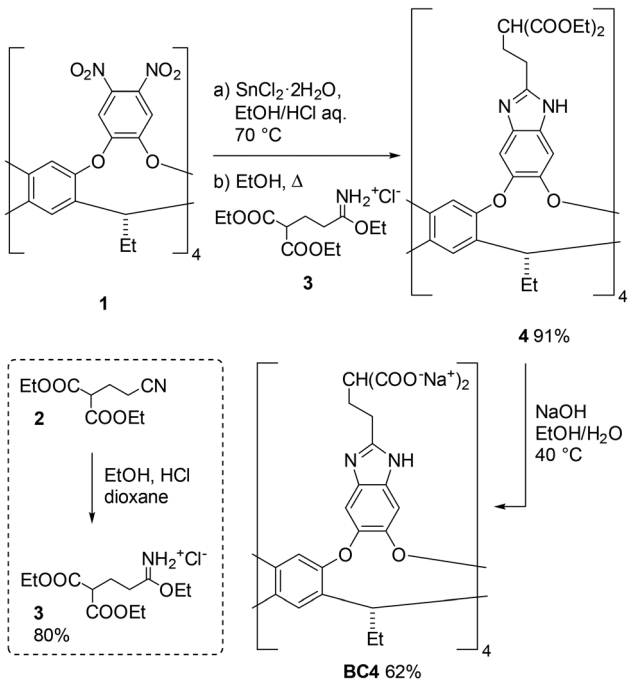

Scheme 1 Synthesis of cavitand **BC4**. Inset: synthesis of imidate precursor **3**.

ble from readily available nitrile **2**, enabling an efficient entry into a novel derivative of the **BC** family, **BC4**. The resulting cavitand would feature 8 carboxylate units, increasing solubility. In addition, the 3-carbon spacer between the core and the hydrophilic rim would significantly deepen the cavity. Receptor **BC4** was synthesized according to Scheme 1. Known octanitro derivative **1** [24] was reduced to the corresponding octaamino hydrochloride salt and subsequently reacted with imidate **3** to furnish octaester cavitand **4**. Upon basic hydrolysis of **4**, sodium octacarboxylate **BC4** was obtained in good yield after dialysis. Importantly, no chromatographic purifications were required throughout this sequence, which can be carried out easily on gram scale.

Receptor **BC4** proved to be completely soluble in pure water at mM concentrations. A 4 mM solution of pure **BC4** has a pH of *ca.* 8. To assess the solubility of **BC4** at varying pH values, solutions of the octacarboxylate salt in D_2O were monitored by ^{1}H NMR upon addition of increasing amounts of DCl ([**BC4**] = 1.3 mM). Remarkably, the cavitand remained completely soluble upon adjusting the pH of the solution down to 4, and resonances assigned to the receptor were clearly observed in the corresponding ^{1}H NMR spectra. At pH < 4 the solution appeared cloudy, indicating precipitation, and no signals from the cavitand could be detected by ^{1}H NMR spectroscopy in these solutions. In contrast, tetracarboxylate **BC1** is only soluble at basic pH (pH ≥ 7.8 or 9 depending on the reports).[8,25]

The spectroscopic features of pure **BC4** in D_2O solution reproduce those previously observed for **BC1–BC3**. Resorcin[4]arene derived cavitands can adopt two extreme conformations, the folded (*vase*) conformer, suitable for binding of guests, or the open (*kite*) conformer.[26] In the absence of a suitable organic guest, the cavitand adopts the kite conformer, as ascertained by the number of resonances observed in the ^{1}H NMR spectrum, corresponding to D_{2d} averaged symmetry (Fig. 2).[27] Kite conformers are postulated to exist as dimers in solution to minimize exposure of the hydrophobic surface to the aqueous media. Upon addition of THF to the aqueous cavitand solution, an abrupt change was observed in the spectrum, indicating the formation of the vase conformer upon binding of THF molecules, despite the accumulation of negatively charged dicarboxylate units that could potentially disfavour folding through repulsive electrostatic interactions. A shift of the methine resonance from 3.96 ppm (D_2O) to 5.53 ppm (D_2O/THF-d_8 95 : 5) is observed, which is diagnostic of the kite-vase transition.[26,28] In addition, the aromatic resonances are shifted downfield and collapse into three resonances, corresponding to the C_{4v} averaged symmetry expected for the vase

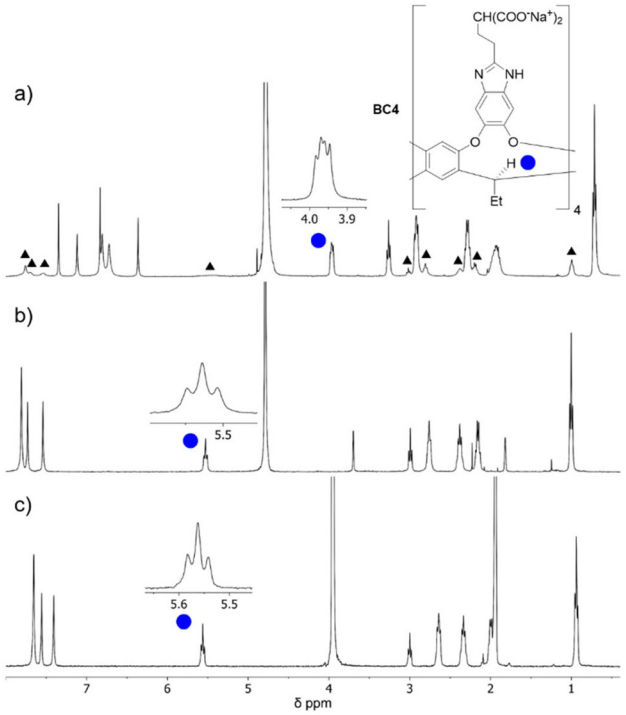

Fig. 2 ^{1}H NMR spectra of **BC4** in different solvents, with the diagnostic methine resonance highlighted (blue dots). (a) D_2O, black triangles indicate small amounts of the vase form, encapsulating residual ethanol. (b) D_2O/THF-d_8 (95 : 5). (c) CD_3CN/D_2O (3 : 1).

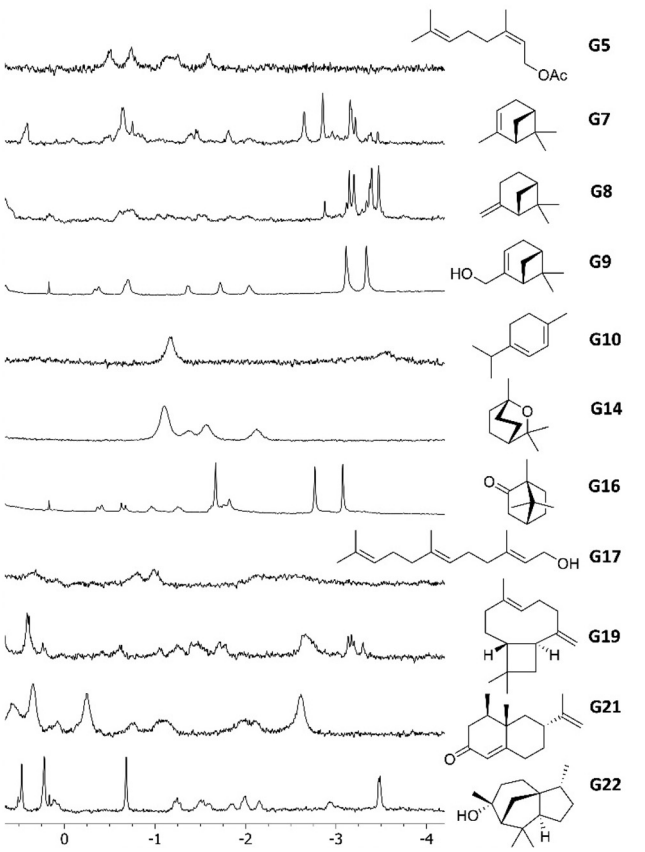

Fig. 3 Far upfield region of the ^{1}H NMR spectra of **BC4** in the presence of different guests, indicating binding in the deep cavity.

conformer. In CD_3CN/D_2O mixtures the vase form is also favoured, despite the fact that the hydrophobic cavity of resorcin[4]arene cavitands typically abhors highly polar molecules.

Having established that the conformational behaviour of **BC4** in aqueous solution is analogous to that of other water-soluble **BCs**, we set out to gauge the binding space of **BC4** by testing its capacity to extract and bind a diverse set of biologically relevant guests in aqueous solutions, including monoterpenes, and sesquiterpenes (**G1–G22**, Fig. 3 and 4). These experiments were carried out at 2 mM concentration of host and excess guest.§ For a number of guests, direct evidence of binding was obtained from the appearance of bound guest signals in the far upfield region of the ^{1}H NMR spectrum—in addition of the characteristic resonances of the *vase* form (Fig. 3). These upfield shifted resonances indicate the formation of complexes that are in slow exchange regime relative to the ^{1}H NMR time-scale, a typical feature of **BC** hosts and related cavitands. For some of these guests, the resonances in the far upfield region are sufficiently resolved to infer directly the guest orientation. For myrtenol (**G9**) and camphor (**G16**) for instance, the appearance of two characteristic singlets that integrate three protons each (relative to the smaller bound guest resonances) is indicative of the *gem*-dimethyl portion of the guest being fixed at the deepest region of the cavity where the magnetic anisotropy is stronger. For α-pinene (**G7**) and β-pinene (**G8**) similar resonances are observed in the same region, although the splitting of these signals indicates that the guest is present in two different orientations under slow exchange kinetics.

Sesquiterpenes are also taken in the cavity as indicated by ^{1}H NMR (**G17**, **G19**, **G21**, **G22**). In the case of cedrol (**G22**) the orientation of the guest can also be deduced: a single methyl resonance around −3.5 ppm indicates that the cyclopentyl ring is oriented towards the deep section of the cavity. This is orientation is reasonable: it places the bulkier bicyclo[3.2.1]octane fragment of **G22** on the wider upper section of the cavitand, exposing at the same time the alcohol function to the aqueous environment and the polar rim of the cavity.

Intriguingly, some of the guests tested triggered the appearance of the *vase* form resonances without evidence of any far upfield shifts, making it impossible to distinguish between specific 1 : 1 binding in the cavity of **BC4** under fast exchange conditions or unspecific interactions outside the cavitand. This was puzzling since the differences of some of these guests with others bound in slow regime are very subtle (*e.g.* **G10** *vs.* **G11–G12**, Fig. 4). This phenomenon has been previously observed with **BC**-type hosts by Rebek.[29] During studies of **BC1** in combination with sodium dodecylsulfate (SDS), it

§ The majority of the guests tested have marginal solubility in pure water. See ESI† for details of the ^{1}H NMR experiments.

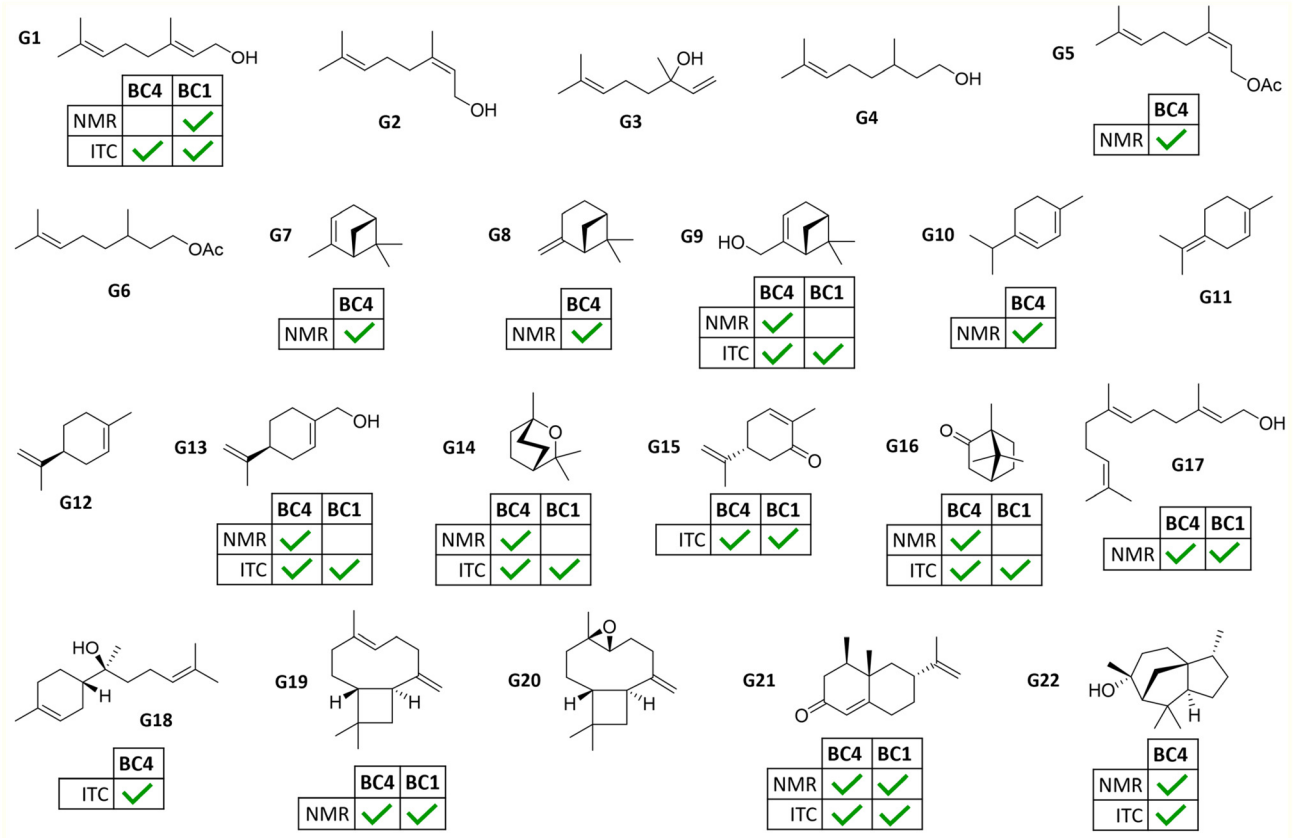

Fig. 4 Guests tested in this study. Green check marks indicate positive evidence of specific binding (1 : 1, slow exchange regime) in the cavity of **BC4** and or **BC1**, respectively.

was reported that above the critical micellar concentration of SDS, **BC1** was found to be in the folded state although no far upfield shifts for bound SDS were observed in the ^{1}H NMR spectrum, indicating that incorporation of **BC** hosts into micelles or similar aggregates enhances guest exchange in and out of the cavity. Given that the barriers to self-exchange in resorcin[4]arene derived cavitands have been determined to be always above 16 kcal mol^{-1}, we assessed the energy barrier associated to the kite-vase transition of **BC4** to understand the observed behaviour. Using an EXSY experiment,[30,31] a Gibbs free energy barrier of 18.2 kcal mol^{-1} was obtained, in good agreement with that obtained for other resorcin[4]arene based cavitands (Fig. S1†).[32] This result suggests that some guests may be able to slip out of the cavity without unfolding or with partial unfolding—for a structurally related cavitand, the calculated exchange barrier to partial opening of one wall is around 15 kcal mol^{-1} in chloroform—[33] and that this slippage mechanism may be favoured when the cavitand is incorporated in micelles or similar aggregates. Fast exchange kinetics may also be the result of poor shape complementarity, as exemplified by the case of geraniol (**G1**). In the presence of **G1**, **BC4** adopts the folded vase conformation but the upfield resonances indicative of slow exchange are not observed. A possible explanation is that **G1** features a narrower shape than the bulkier polycyclic monoterpenes (**G7–G9**, **G14**, **G16**), significantly reducing the available attractive contacts with the hydrophobic cavity. Structurally related farnesol (**G17**) appears to bind in the cavity, but the broad upfield shifts observed also suggest that the guest is on the verge of fast chemical exchange (Fig. 3).

For completeness, we assessed the inclusion of guests in receptor **BC1** under the same conditions (Fig. 5). Somewhat surprisingly, both geraniol and farnesol bind in slow exchange regime within cavitand **BC1**, providing well resolved resonances that indicate the encapsulation of the terminal *gem*-dimethyl groups at the deepest section of the host. Evidence of internalization was also obtained for caryophyllene (**G19**), nootkatone (**G21**) and cedrol (**G22**).

Considering the previous findings and in order to establish a systematic comparison between the binding abilities of **BC4** and **BC1** that is not blurred by exchange kinetics, we evaluated the association constants (K_a) for a representative selection of guests by isothermal titration calorimetry (ITC, Table 1 and ESI†). The selected guests were chosen to provide sufficient solubility in aqueous solution. We were able to fit the obtained calorimetric data to 1 : 1 stoichiometry isotherms, confirming the formation of well-defined inclusion complexes as opposed to unspecific binding on the outside of the host. With the exception of geraniol, all the guests tested provided increased affinity for **BC4**, with association constants up to one order of

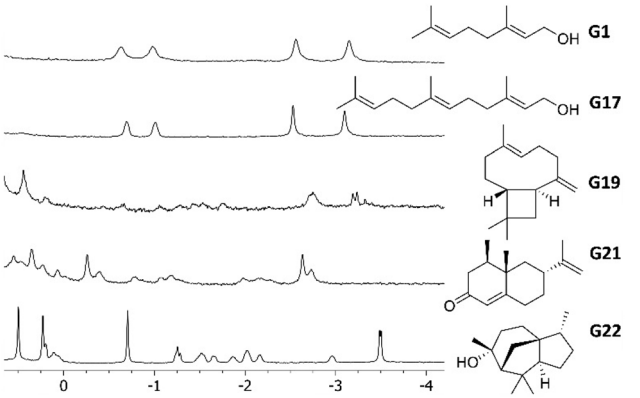

Fig. 5 ^{1}H NMR evidenced for the 1 : 1 encapsulation of different guests within host **BC1** in D_2O at 25 °C.

Table 1 Association constants (K_a) of different guests with **BC4** and **BC1**[a]

Entry	Guest	K_a (**BC4**) M^{-1}	K_a (**BC1**) M^{-1}
1	**G1**	$1.62 \pm 0.04 \times 10^5$	$1.22 \pm 0.04 \times 10^5$
2	**G9**	$2.91 \pm 0.05 \times 10^5$	$1.23 \pm 0.05 \times 10^5$
3	**G13**	$1.19 \pm 0.04 \times 10^6$	$3.7 \pm 0.2 \times 10^5$
4	**G14**	$9.9 \pm 0.2 \times 10^3$	$2.0 \pm 0.1 \times 10^3$
5	**G15**	$1.06 \pm 0.01 \times 10^6$	$5.5 \pm 0.3 \times 10^5$
6	**G16**	$9.5 \pm 0.4 \times 10^4$	$3.9 \pm 0.2 \times 10^4$
7	**G18**	$1.5 \pm 0.1 \times 10^5$	—[b]
8	**G21**	$1.34 \pm 0.04 \times 10^5$	$5.0 \pm 0.2 \times 10^4$

[a] Determined by ITC at 25 °C in H_2O (5% v/v EtOH). [b] Not determined due to the low magnitude of K_a and solubility constraints.

magnitude above those obtained for **BC1**. For bisabolol (**G18**), the association constant with **BC1** could not be properly measured because of solubility constraints, indicating qualitatively an important reduction in affinity with respect to **BC4**.

To better understand the previous results, we carried out computational modelling of a selection of complexes with **BC4** and **BC1** as the sodium salts, including 4 water bridging molecules (Fig. 6 and S2†). The spaces between carboxylate units from adjacent panels of the cavitand provide a good fit for sodium cations. The resulting saline bridges stabilize the vase conformation, which explains the fact that **BC4** retains the preference for the vase conformer observed in **BC1–3** despite the accumulation of carboxylate units at the upper rim. The different exchange kinetics observed correlate qualitatively with the shape complementarity between host and guest.

Polycyclic monoterpenes (**G7-G8, G14, G16**) feature a spherical shape that is very complementary to the lower half of the cavitand surface, maximizing attractive non-covalent interactions with the aromatic panels (Fig. 6). On the contrary, acyclic terpenes favour extended conformations of narrower shape and poorer complementarity, resulting in a reduction of the available attractive interactions with the cavitand's wall.[22] A possible explanation for the binding of geraniol in **BC1** under slow exchange regime can be derived from the corresponding

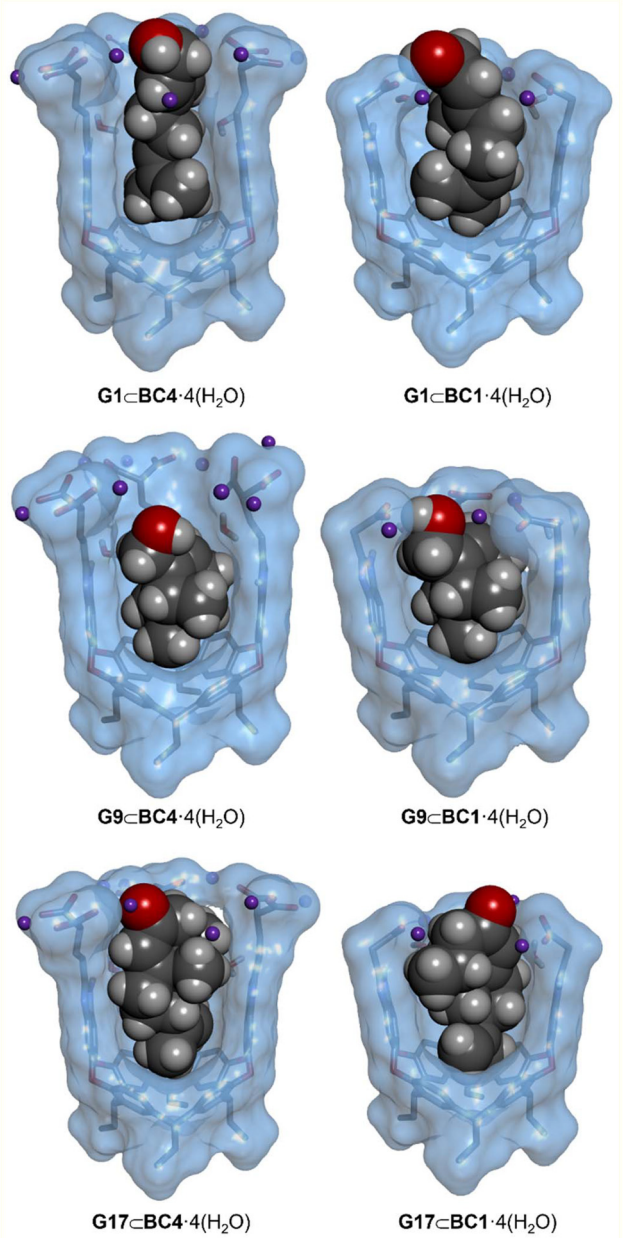

Fig. 6 Molecular models of geraniol (**G1**), myrtenol (**G9**) and nootkatone (**G17**) bound in **BC4**·4(H_2O) and **BC1**·4(H_2O) (MMFF). The cavitands are shown with a superimposed solvent accessible surface (front panel omitted for clarity) illustrating the different degrees of host–guest complementarity along the guest series. Sodium ions are shown as purple spheres.

molecular model. Geraniol engages in hydrogen bonding with the carboxylates on the rim of the cavitands, forcing the adoption of a contorted and more complementary conformation, enhancing interactions with the cavitand walls. A similar phenomenon can be invoked for farnesol (**G17**). Conversely, the carboxylate functions of **BC4** are farther apart from the deep section of the cavity, so that hydrogen bonding to **G1** favours the less complementary extended conformation that ensures exposure of the hydroxyl group to the aqueous medium.

Molecular modelling also provides a reasonable explanation for the enhanced binding constants of cyclic terpenes in **BC4**. As it can be observed in Fig. 6, the binding of terpenes in **BC1** leads to a slight distortion of the walls towards the exterior in comparison to **BC4**. This "bloating" of the cavitand results in less efficient bridging by the auxiliary water molecules—the hydrogen bonding interactions are stretched. The net effect in terms of association constants is subtle for monoterpenes (Table 1, entry 2), but the higher complementarity of cyclic sesquiterpenes with **BC4** is evident in the complex with nootkatone (**G21**). The most likely orientation of the guest is that with the isopropylidene group positioned in the narrow, tapered end of the receptor, and the bulkier cyclohexenone portion accommodated in the wider upper region defined by the ethylene spacers of **BC4**, providing additional van der Waals interactions that are not available in **BC1**. A similar effect can be appreciated in the complexes of bisabolol, caryophyllene, and cedrol (Fig. S2†). For caryophyllene (**G19**) and cedrol (**G22**) the bulkier *E*-cyclonene and bicyclo[3.2.1]octane fragments respectively provide good complementarity with the wider upper region of **BC4** defined by the ethylene spacers.

Conclusions

In summary, we have developed a new benzimidazole-type cavitand based on resorcin[4]arene (**BC4**) that expands and complements the capabilities of the existing family of **BC** receptors. **BC4** presents and improved solubility profile, operating in a wider range of pH. In addition, **BC4** presents an expanded hydrophobic cavity that allows enhanced binding of sizable guests such as sesquiterpenes, while preserving the affinity towards smaller guests typical of analogue **BC1**. The guest exchange kinetics are very sensitive to subtle changes in shape size and shape. **BC4** is readily available on gram scale and requires no chromatographic purifications. Overall, all these features bode well for the implementation of **BC4** in sensing applications of biologically relevant analytes.

Data availability

The data supporting the findings reported in this manuscript has been deposited in the CORA.RDR institutional repository, **DOI: 10.34810/data1632**.

The dataset contains raw and processed data in the following categories:

Full NMR characterization data for new compounds.

^{1}H NMR data for the binding studies reported.

Optimized geometries and optimization files for the computational studies reported.

Conflicts of interest

There are no conflicts to declare.

Acknowledgements

We are grateful for financial support from grants PID2020-113181GB-I00, TED2021-130573B-I00, PID2023-146498NB-I00, and REQ2021_B_05 funded by MICIU/AEI/10.13039/501100011033 and by the European Union NextGenerationEU/PRTR. We thank AGAUR/Generalitat de Catalunya for funding (2021SGR623) and for a pre-doctoral fellowship to R. L. (2020 FI_B 00132). Open Access funding provided thanks to the CRUE-CSIC agreement with the RSC.

References

1 M. A. Beatty and F. Hof, Host–guest binding in water, salty water, and biofluids: general lessons for synthetic, bio-targeted molecular recognition, *Chem. Soc. Rev.*, 2021, **50**, 4812–4832.

2 J. Murray, K. Kim, T. Ogoshi, W. Yao and B. C. Gibb, The aqueous supramolecular chemistry of cucurbit[n]urils, pillar[n]arenes and deep-cavity cavitands, *Chem. Soc. Rev.*, 2017, **46**, 2479–2496.

3 A. R. Far, A. Shivanyuk and J. Rebek, Water-Stabilized Cavitands, *J. Am. Chem. Soc.*, 2002, **124**, 2854–2855.

4 F. R. Pinacho Crisóstomo, A. Lledó, S. R. Shenoy, T. Iwasawa and J. Rebek Jr., Recognition and Organocatalysis with a Synthetic Cavitand Receptor, *J. Am. Chem. Soc.*, 2009, **131**, 7402–7410.

5 R. J. Hooley, H. J. Van Anda and J. Rebek, Cavitands with Revolving Doors Regulate Binding Selectivities and Rates in Water, *J. Am. Chem. Soc.*, 2006, **128**, 3894–3895.

6 C. H. Haas, S. M. Biros and J. J. Rebek, Binding properties of cavitands in aqueous solution—the influence of charge on guest selectivity, *Chem. Commun.*, 2005, 6044–6045.

7 L. Trembleau and J. Rebek, Helical Conformation of Alkanes in a Hydrophobic Cavitand, *Science*, 2003, **301**, 1219–1220.

8 F. Hof, L. Trembleau, E. C. Ullrich and J. J. Rebek, Acetylcholine Recognition by a Deep, Biomimetic Pocket, *Angew. Chem., Int. Ed.*, 2003, **42**, 3150–3153.

9 Y.-Q. Chen, H.-W. Guan, K. Kanagaraj, J. Rebek and Y. Yu, Metal coordination to a deep cavitand promotes binding selectivities in water, *Chin. Chem. Lett.*, 2022, **33**, 4908–4911.

10 Y. Zhu, M. Tang, H. Zhang, F.-U. Rahman, P. Ballester, J. Rebek Jr., C. A. Hunter and Y. Yu, Water and the Cation–π Interaction, *J. Am. Chem. Soc.*, 2021, **143**, 12397–12403.

11 H.-W. Guan, Y.-J. Zhu, J. Peters, O. Brea, F. Himo, J. Rebek and Y. Yu, Recognition of hydrophilic molecules in deep cavitand hosts with water-mediated hydrogen bonds, *Chem. Commun.*, 2021, **57**, 8147–8150.

12 A. D. Gill, B. L. Hickey, W. Zhong and R. J. Hooley, Selective sensing of THC and related metabolites in biofluids by host:guest arrays, *Chem. Commun.*, 2020, **56**, 4352–4355.

13 Y. Liu, A. D. Gill, Y. Duan, L. Perez, R. J. Hooley and W. Zhong, A supramolecular sensor array for selective immunoglobulin deficiency analysis, *Chem. Commun.*, 2019, **55**, 11563–11566.
14 A. D. Gill, L. Perez, I. N. Q. Salinas, S. R. Byers, Y. Liu, B. L. Hickey, W. Zhong and R. J. Hooley, Selective Array-Based Sensing of Anabolic Steroids in Aqueous Solution by Host–Guest Reporter Complexes, *Chem. – Eur. J.*, 2019, **25**, 1740–1745.
15 Y. Liu, J. Lee, L. Perez, A. D. Gill, R. J. Hooley and W. Zhong, Selective Sensing of Phosphorylated Peptides and Monitoring Kinase and Phosphatase Activity with a Supramolecular Tandem Assay, *J. Am. Chem. Soc.*, 2018, **140**, 13869–13877.
16 Y. Liu, Y. Duan, A. D. Gill, L. Perez, Q. Jiang, R. J. Hooley and W. Zhong, Metal-assisted selective recognition of biothiols by a synthetic receptor array, *Chem. Commun.*, 2018, **54**, 13147–13150.
17 Y. Liu, L. Perez, A. D. Gill, M. Mettry, L. Li, Y. Wang, R. J. Hooley and W. Zhong, Site-Selective Sensing of Histone Methylation Enzyme Activity via an Arrayed Supramolecular Tandem Assay, *J. Am. Chem. Soc.*, 2017, **139**, 10964–10967.
18 Y. Liu, M. Mettry, A. D. Gill, L. Perez, W. Zhong and R. J. Hooley, Selective Heavy Element Sensing with a Simple Host–Guest Fluorescent Array, *Anal. Chem.*, 2017, **89**, 11113–11121.
19 Y. Liu, L. Perez, M. Mettry, C. J. Easley, R. J. Hooley and W. Zhong, Self-Aggregating Deep Cavitand Acts as a Fluorescence Displacement Sensor for Lysine Methylation, *J. Am. Chem. Soc.*, 2016, **138**, 10746–10749.
20 R. J. Hooley, S. M. Biros and J. Rebek Jr, A Deep, Water-Soluble Cavitand Acts as a Phase-Transfer Catalyst for Hydrophobic Species, *Angew. Chem., Int. Ed.*, 2006, **45**, 3517–3519.
21 Y.-J. Ghang, M. P. Schramm, F. Zhang, R. A. Acey, C. N. David, E. H. Wilson, Y. Wang, Q. Cheng and R. J. Hooley, Selective Cavitand-Mediated Endocytosis of Targeted Imaging Agents into Live Cells, *J. Am. Chem. Soc.*, 2013, **135**, 7090–7093.
22 A. Lledó and A. Soler, Binding of ion pairs in a thiourea-functionalized self-folding cavitand, *Org. Chem. Front.*, 2017, **4**, 1244–1249.
23 M. Mettry, M. P. Moehlig and R. J. Hooley, Synthesis, Guest Binding, and Metal Coordination of Functionalized Self-Folding Deep Cavitands, *Org. Lett.*, 2015, **17**, 1497–1500.
24 P. Amrhein, A. Shivanyuk, D. W. Johnson and J. Rebek, Metal-Switching and Self-Inclusion of Functional Cavitands, *J. Am. Chem. Soc.*, 2002, **124**, 10349–10358.
25 S. M. Biros, E. C. Ullrich, F. Hof, L. Trembleau and J. Rebek, Kinetically Stable Complexes in Water: The Role of Hydration and Hydrophobicity, *J. Am. Chem. Soc.*, 2004, **126**, 2870–2876.
26 J. R. Moran, J. L. Ericson, E. Dalcanale, J. A. Bryant, C. B. Knobler and D. J. Cram, Vases and kites as cavitands, *J. Am. Chem. Soc.*, 1991, **113**, 5707–5714.
27 R. J. Hooley, H. J. Van Anda and J. Rebek, Extraction of Hydrophobic Species into a Water-Soluble Synthetic Receptor, *J. Am. Chem. Soc.*, 2007, **129**, 13464–13473.
28 T. Haino, D. M. Rudkevich, A. Shivanyuk, K. Rissanen and J. J. Rebek, Induced-Fit Molecular Recognition with Water-Soluble Cavitands, *Chem. – Eur. J.*, 2000, **6**, 3797–3805.
29 L. Trembleau and J. Rebek Jr, Interactions between a surfactant and cavitand in water blur distinctions between host and guest, *Chem. Commun.*, 2004, 58–59.
30 K. Nikitin and R. O'Gara, Mechanisms and Beyond: Elucidation of Fluxional Dynamics by Exchange NMR Spectroscopy, *Chem. – Eur. J.*, 2019, **25**, 4551–4589.
31 C. L. Perrin and T. J. Dwyer, Application of two-dimensional NMR to kinetics of chemical exchange, *Chem. Rev.*, 1990, **90**, 935–967.
32 A. Lledó and J. Rebek Jr, Deep cavitand receptors with pH-independent water solubility, *Chem. Commun.*, 2010, **46**, 8630–8632.
33 R. López-Coll, R. Álvarez-Yebra, F. Feixas and A. Lledó, Comprehensive Characterization of the Self-Folding Cavitand Dynamics, *Chem. – Eur. J.*, 2021, **27**, 10099–10106.

